All-spectrum Cognitive Channelization around Narrowband and Wideband Primary Stations

George Sklivanitis,* Emrecan Demirors,† Adam M. Gannon,* Stella N. Batalama,*
Dimitris A. Pados,* and Tommaso Melodia†
*Department of Electrical Engineering, The State University of New York at Buffalo, Buffalo, NY 14260-2050.
E-mail:{gsklivan, adamgann, batalama, pados}@buffalo.edu
†Department of Electrical and Computer Engineering, Northeastern University, Boston, MA 02115.
E-mail:{edemirors, melodia}@ece.neu.edu

***Abstract*—In this paper we design, implement, and experimentally evaluate a wireless software-defined radio platform for cognitive channelization in the presence of narrowband or wideband primary stations. Cognitive channelization is achieved by jointly optimizing the transmission power and the waveform channel of the secondary users. The process of joint resource allocation requires no a-priori knowledge of the transmission characteristics of the primary user and maximizes the signal-to-interference-plus-noise ratio (SINR) at the output of the secondary receiver. This is achieved by designing waveforms that span the whole continuum of available/device-accessible spectrum, while satisfying a peak power constraint for the secondary users and an interference temperature (IT) constraint for the primary users. We build a four-node software-defined radio testbed and experimentally demonstrate in an indoor laboratory environment the theoretical concepts of all-spectrum cognitive channelization in terms of pre-detection SINR and bit-error-rate (BER) at both primary and secondary receivers.**

***Index Terms*—Cognitive underlay network, all-spectrum channelization, software-defined radio, testbed implementation**

I. Introduction

Cognitive Radio (CR) has emerged as a promising technology for improving spectrum utilization efficiency [1]–[4]. In this paper we are interested in the deployment of secondary links that operate in "gray spaces" and coexist with unknown narrowband [5] or wideband primary stations [6]–[8]. Contrary to conventional cognitive radio proposals [9], [10] where secondary users sense the whole spectrum for available/void only frequency bands, all-spectrum cognitive channelization considers secondary users that operate concurrently in frequency and time with primary users in an underlay fashion. This is achieved by optimizing the transmission power and waveform channel of the secondary users in a way that satisfies pre-defined interference temperature constraints at the primary receiver, while at the same time maximizes the signal-to-interference-plus-noise ratio (SINR) at the output of the secondary receiver. The novelty of the all-spectrum cognitive channelization approach originates from the treatment of all-hardware accessible frequency spectrum, space, and time as a unified resource to be dynamically managed according to intra- and inter-network interference conditions.

Different paradigms for shared access such as overlay, underlay, and interweave are described in [11]. Underlay paradigms have been extensively investigated in the literature using analytical tools and simulation platforms, however their hardware realization is yet quite challenging. For example, past work in the field of all-spectrum cognitive channelization investigated the design of maximum SINR secondary wideband links that cooperate [6], [7] or simply coexist without any form of cooperation [8] with primary wideband users, while at the same time satisfy the quality-of-service (QoS) requirements for both the primary and the secondary links. In [5] a joint resource allocation and admission control algorithm is proposed to minimize the total energy consumption in a secondary code-division network coexisting with a narrowband primary system. In the context of multiple-antenna cognitive underlay secondary links, the work in [12], [13] exploits information exchange in the primary feedback control channel and proposes effective cognitive beamforming and interference avoidance algorithms, while the work in [14] describes an experimental prototype for multiple-input-multiple-output (MIMO) cognitive beamforming. Experimental work for spectral coexistence of wideband networks and narrowband stations in unlicensed "white-spaces" (unused spectrum bands) is presented in [15] and [16], respectively.

In this manuscript we present a practical deployment of all-spectrum cognitive channelization in a four-node software-defined radio (SDR) testbed. More specifically, we design and implement cognitive transmitter and receiver architectures that experimentally demonstrate the theoretical concepts of channelization in the presence of unknown primary users (i.e. narrowband or wideband). Within this context, we present an integrated complete hardware/software implementation of the secondary system and address comprehensively implementation challenges related to frame detection, carrier frequency and time synchronization, multipath channel estimation, and maximum-SINR filtering in the presence of primary users. In addition, we design and implement an adaptive scheme for optimizing the transmission waveform and power at the secondary transmitter that ensures QoS requirements both at the primary user and at the secondary link. The proposed algorithm provides a suboptimal solution to a well-known non-convex NP-hard optimization problem, and offers a methodology to experimentally realize the performance enhancements of cognitive channelization. The capabilities of the proposed experimental testbed of a complete cognitive SDR system operating in "gray spaces" are demonstrated in terms of SINR and bit-error-rate (BER) performance at both the primary and the secondary receivers.

In summary, our objective is to provide a comprehensive system design for experimental evaluation of all-spectrum cognitive channelization on a SDR testbed. We present an integrated complete hardware/software implementation of the

978-1-4799-5952-5/15/$31.00 ©2015 IEEE

secondary receiver and address design challenges that arise in deployment conditions of the integrated system and are usually absent in simulation-based implementations of specific parts of the system components [17], [18].

The rest of the paper is organized as follows. In Section II, we introduce the system model. Section III presents secondary receiver considerations and Section IV discusses the specifics of the cognitive channelization algorithm. Section V describes the SDR testbed setup and provides experimental results that demonstrate the performance of the proposed cognitive scheme. A few concluding remarks are drawn in Section VI.

II. System Model

We consider the design and implementation of a secondary link (secondary transmitter-receiver pair) operating on the same frequency band and concurrently with a primary station (Fig. 1). The secondary user transmits binary antipodal information symbols $b_s(i) \in \{\pm 1\}$, $i = 0, \ldots, J-1$ at rate $1/T$, modulated by a signal waveform $d_s(t)$ of duration T. If f_c denotes the common carrier frequency, then the transmitted signal of the secondary user *STx* can be expressed as

$$x_s(t) = \sum_{i=0}^{J-1} b_s(i)\sqrt{E_s}d_s(t-iT)e^{j(2\pi f_c t+\phi_s)}, \qquad (1)$$

where $E_s > 0$ denotes transmitted energy per bit and ϕ_s is the receiver carrier phase relative to the secondary transmitter's local oscillator. The information symbols $b_s(i)$ are modulated by a distinct digital waveform $d_s(t)$ given by

$$d_s(t) = \sum_{l=0}^{L-1} s_s(l) g_{T_d}(t - lT_d), \qquad (2)$$

where $s_s(l) \in \frac{1}{\sqrt{L}}\{\pm 1\}$ is the l-th waveform-bit of the digital waveform assigned to the secondary transmitter, $g_{T_d}(\cdot)$ is a pulse shaping square-root-raised-cosine (SRRC) filter of duration T_d, and $T = LT_d$ is the waveform duration (period).

The transmitted signal of primary users PTx_k, $k = 1, \ldots, K$ can be expressed as

$$x_p(t) = \sum_{i=0}^{J-1} b_p(i)\sqrt{E_p}d_p(t-iT)e^{j(2\pi f_c t+\phi_p)}, \qquad (3)$$

where $b_p(i) \in \{\pm 1\}$ are the transmitted information symbols, $E_p > 0$ is the bit energy, f_c denotes the common carrier frequency, and ϕ_p is the corresponding carrier phase. For the narrowband case, $d_p(t) = g_T(t)$ is a SRRC pulse shaper, while for the all-spectrum wideband case $d_p(t) = \sum_{l=0}^{L-1} s_p(l) g_{T_d}(t - lT_d)$ denotes the digital waveform with $s_p(l) \in \frac{1}{\sqrt{L}}\{\pm 1\}$, and $T_d = T/L$.

All signals are considered to propagate over Rayleigh multipath fading channels and experience complex additive white Gaussian noise (AWGN) at the receiver. Multipath fading is modeled by a linear tapped-delay line with taps that are spaced at T_d intervals and are weighted by independent fading coefficients. We note that low-cost, commodity transceivers commonly introduce carrier frequency offsets Δf, between transmitter-receiver pairs, mainly due to the radios' clock crystal instabilities and inaccuracies introduced by the manufacturing process. Therefore, the received baseband signal

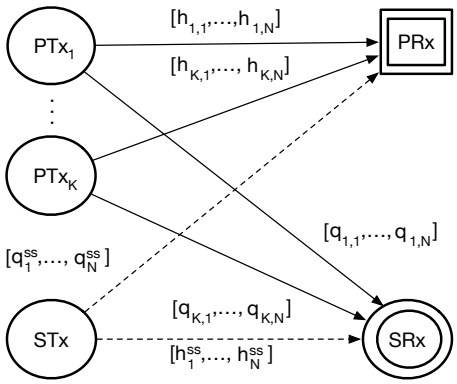

Fig. 1. Primary/secondary cognitive underlay system model of K primary transmitters PTx_k, $k = 1, \ldots, K$, a primary receiver PRx, and a secondary transmitter-receiver pair *STx-SRx*.

at the secondary receiver *SRx* after carrier demodulation is modeled appropriately by

$$r(t) = \sum_{i=0}^{J-1} b_s(i) \sum_{n=0}^{N-1} \sqrt{E_s}\tilde{h}_n^{ss} d_s(t - iT - nT_d - \tau^{ss}) \cdot e^{-j2\pi\Delta f t} + i(t) + n(t) \qquad (4)$$

where N denotes the total number of resolvable paths, and $\tilde{h}_n^{ss} = h_n^{ss} e^{-j(2\pi f_c n T_d + 2\pi f_c \tau_n^{ss} - \phi_s)}$ are the complex baseband channel coefficients with h_n^{ss}, $n = 0, \ldots, N-1$, modeled as independent zero-mean complex Gaussian random variables that remain constant over T_d, τ_n^{ss} denotes comprehensively the transmission and multipath propagation delay of the n-th path, while $i(t)$ and $n(t)$ model primary users transmissions and additive noise, respectively.

III. Secondary Receiver Design

In this section we present system design considerations related to frame detection, carrier frequency offset compensation, symbol time synchronization, channel estimation and maximum SINR filtering of the received signal at the secondary receiver in the presence of narrowband or wideband primary users. We focus on low-complexity software-defined receivers that can effectively address system design issues that arise in a real-world deployment of a cognitive software-radio.

A typical SDR platform consists of an analog front-end that is responsible for up/down-conversion of digital baseband/analog information signals and includes low-pass/bandpass filters, mixers and amplifiers for signal conditioning. The analog front-end interfaces with high sample rate analog-to-digital (AD)/digital-to-analog (DA) converters that sample analog/digital waveforms for reception/transmission. Baseband processing usually takes place either in a field-programmable-gate-array (FPGA) or a host-PC via a high-speed data bus.

A. Frame Detection

Assuming frame-based transmissions from both primary and secondary users, we adopt the philosophy of a low-complexity frame detection technique, widely employed in WLAN-based protocols [19]. However, contrary to the repeating pattern of short-preamble training sequences [19], [20] we exploit

the autocorrelation properties of the digital waveform $d_s(t)$ (known a-priori at the receiver). The frame structure of the secondary link is summarized in Fig. 2. The first P bits of each frame are unmodulated (i.e. equal to 1) which implies that the first P replicas of the digital waveform $d_s(t)$ are also unmodulated.

Let $f_s = \frac{1}{T_s}$ and $I = \frac{T_d}{T_s}$ be the secondary receiver's sampling rate and the number of samples per code-bit used for interpolation at *STx*, respectively. Then, for the k-th received sample from the AD converter, $r[k] \triangleq r(kT_s)$ we implement a moving average over a variable window P_{win} as follows

$$R[k] = \sum_{m=0}^{P_{\text{win}}-1} r[k+m] r^* [k+m+LI] . \tag{5}$$

We conducted several experiments and found that a window of size $P_{\text{win}} \simeq 6\% \cdot P \cdot L \cdot I$ (i.e. 6% of the preamble's training samples) performs well in the presence of multiple primary users signals. By defining the average power of the k-th received sample, as $P[k] \triangleq \sum_{m=0}^{P_{\text{win}}-1} |r[k+m]|^2$, the following frame timing metric is independent of the power level of the received samples:

$$W[k] \triangleq \frac{|R[k]|}{P[k]}. \tag{6}$$

In our implementation we identify beginning of a frame if $W[k] > \Theta$ for a number of consecutive samples and for a user-defined threshold $\Theta \in [0, 1]$. We note that in the absence of intersymbol interference (ISI) and multiple-access interference (MAI), $W[k]$ reaches a plateau that extends over $P \cdot L \cdot I$ samples.

B. Carrier Frequency Offset Estimation and Compensation

After we acquire the beginning of a frame, we need to compensate for the frequency offset created by the mismatch between the clock oscillators of both the *STx-SRx* and PTx_k-*SRx*, $k = 1, \ldots, K$ pairs. A quality estimate $\widehat{\Delta f}$, can be obtained by exploiting the pattern of the $P \cdot L \cdot I$ preamble training samples as in [21], which results in the following simple waveform-bit-level-correlation frequency offset estimator

$$\widehat{\Delta f} = \frac{1}{2\pi LI} \angle \sum_{i=0}^{(P-1)LI-1} r[i] r^* [i+LI] . \tag{7}$$

We can therefore compensate for the frequency offset in the acquired frame (provided that Δf is constant over a frame duration) by applying $\widehat{\Delta f}$ to the k-th received sample as follows

$$y[k] \triangleq y(kT_s) = r(kT_s) \exp(j2\pi \widehat{\Delta f} kT_s). \tag{8}$$

C. Symbol Time Synchronization

The received samples $y[k]$ are now ready for pulse matched filtering and sampling at rate $1/T_d$ over the multipath extended symbol period of $L + N - 1$ waveform-bits. After discarding the first P preamble bits, the received data

$$\mathbf{y} = \begin{bmatrix} y[\tau_0] \\ y[\tau_0 + I] \\ \vdots \\ y[\tau_0 + ((J-P)L + N - 2)I] \end{bmatrix} \in \mathbb{C}^{((J-P)L+N-1)\times 1} \tag{9}$$

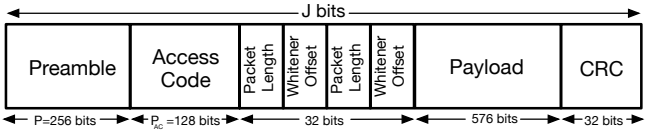

Fig. 2. Frame structure for the *STx-SRx* secondary link.

are ready for maximum SINR filtering and detection of the information bits of the secondary user $b_s(i), i = 0, \ldots, J-P-1$. However, there is a timing uncertainty regarding the sample $y[k]$ that corresponds to the beginning of the first symbol. In our testbed implementation we address this problem by allocating at each frame header a number of training access code bits denoted by P_{AC}. Then, $\tau_0 \in [0, P_{AC}LI)$, $P_{AC} \in \mathbb{Z}$. The estimate for τ_0 is acquired by calculating and buffering all possible $(P_{AC}L)$-shifted crosscorrelation matrices

$$\mathbf{R}^{(l)} = \mathrm{E}\{\mathbf{y}_{\mathrm{i}}^{(l)} \mathbf{y}_{\mathrm{AC_i}}^{\mathrm{H}}\}, \quad \mathrm{l} = 0, \ldots, \mathrm{P_{AC}L} - 1 \tag{10}$$

where

$$\mathbf{y}_i^{(l)} = \begin{bmatrix} y[(iL+l)I] \\ y[(iL+l+1)I] \\ \vdots \\ y[(i+1)L+N+l-2)I] \end{bmatrix}, \quad i = 0, \ldots, J-P-1, \tag{11}$$

and

$$\mathbf{y}_{AC_i} = \begin{bmatrix} b_s(P+i)s_s(0) \\ \vdots \\ b_s(P+i)s_s(L-1) \end{bmatrix}, \quad i = 0, \ldots, P_{AC}-1, \tag{12}$$

and $\mathbf{y}_{AC_i} = [0 \quad \ldots \quad 0]^T$, for $i = P_{AC}, \ldots, J-P-1$.

Then, the beginning of the first symbol is obtained as in [18]

$$\hat{\tau}_0 = \arg \max_{l \in \{0,\ldots,P_{AC}L-1\}} \left\{ ||\mathbf{R}^{(l)}||^2 \right\}. \tag{13}$$

Given $\hat{\tau}_0$ and with respect to the i-th bit, we can re-write the received data vector after chip-matched filtering and sampling at the chip rate $1/T_d$ in the following form

$$\mathbf{y}_i = [\mathbf{y}]_{((\hat{\tau}_0+iL)I):I:((\hat{\tau}_0+L+N-2+iL)I)} , \tag{14}$$

which is equivalent to

$$\mathbf{y}_i = \sqrt{E_s} b_s(P+i) \mathbf{H}^{ss} \mathbf{s}_s + \mathbf{p}_i + \mathbf{n}_i, \quad i = 0, \ldots, J-P-1 \tag{15}$$

where $\mathbf{H}^{ss} \in \mathbb{C}^{(L+N-1)\times L}$ is the multipath fading channel matrix given as follows

$$\mathbf{H}^{ss} = \sum_{n=0}^{N-1} \tilde{h}_n^{ss} \begin{bmatrix} \mathbf{0}_{n\times L} \\ \mathbf{I}_{L\times L} \\ \mathbf{0}_{(N-n-1)\times L} \end{bmatrix}. \tag{16}$$

We assume that $\mathbf{n}_i \sim \mathcal{CN}(\mathbf{0}, \sigma_n^2 \mathbf{I}_{L+N-1})$ represents complex zero-mean white Gaussian noise, while $\mathbf{p}_i$ accounts for the unknown primary users signals.

D. Channel Estimation

To estimate the channel coefficients $\mathbf{h}^{ss} = \left[\tilde{h}_1^{ss}, \ \tilde{h}_2^{ss}, \ \ldots \ \tilde{h}_N^{ss}\right]^T$ for the secondary user of interest we resort to the training access code bits P_{AC}. We re-write (15) as follows

$$\mathbf{y}_i = \sqrt{E_s} b_s(P+i)\mathbf{S}_s\mathbf{h}^{ss} + \mathbf{p}_i + \mathbf{n}_i, \quad i = 0, \ldots, J-P-1 \tag{17}$$

where $\mathbf{S}_s$ is the channel processed waveform matrix

$$\mathbf{S}_s \triangleq \begin{bmatrix} s_s(1) & & \mathbf{0} \\ & \ddots & \vdots \\ \vdots & & s_s(1) \\ s_s(L) & & \vdots \\ & \ddots & \\ \mathbf{0} & & s_s(L) \end{bmatrix}_{(L+N-1)\times N}. \tag{18}$$

We estimate the (scaled) channel coefficients by averaging the input vectors $\mathbf{y}_i$ over the known access code bits $b_s(P+i)$, $i = 0, \ldots, P_{AC}-1$, ([8]) i.e.

$$\widehat{\sqrt{E_s}\mathbf{h}}^{ss} = (\mathbf{S}_s^H\mathbf{S}_s)^{-1}\mathbf{S}_s^H \frac{1}{P_{AC}} \sum_{i=0}^{P_{AC}-1} \mathbf{y}_i b_s^*(P+i), \tag{19}$$

and we create a matrix channel estimate $\widehat{\mathbf{H}}^{ss}$ by (16).

E. Maximum SINR RAKE Filtering

Maximum SINR RAKE filtering takes advantage of both the RAKE principle that exploits the N received paths as well as the theory of linearly constrained minimum variance filters [22], [23]. The work in [24] finds the finite-impulse-response (FIR) filter $\mathbf{w}$ that minimizes the energy at the output of the filter subject to the constraint that the output of the multipath channel for the secondary user of interest remains constant, (e.g. $\mathbf{w}^H\mathbf{w}_{||\mathrm{R-MF}||} = 1$) where

$$\mathbf{w}_{\mathrm{R-MF}} \stackrel{\triangle}{=} \widehat{\mathbf{H}}^{ss}\mathbf{s}_s, \qquad \mathbf{w}_{||\mathrm{R-MF}||} \stackrel{\triangle}{=} \frac{\mathbf{w}_{\mathrm{R-MF}}}{||\mathbf{w}_{\mathrm{R-MF}}||} \tag{20}$$

are the $(L+N-1)$-tap RAKE-matched-filter (MF) and its normalized version, respectively. The solution to this optimization problem results in the minimum-variance-distortionless-response (MVDR) or, equivalently, maximum-SINR filter structure given by the following expression

$$\mathbf{w}_{\mathrm{maxSINR}} \stackrel{\triangle}{=} \frac{\widehat{\mathbf{R}}^{s^{-1}}\mathbf{w}_{||\mathrm{R-MF}||}}{\mathbf{w}_{||\mathrm{R-MF}||}^H\widehat{\mathbf{R}}^{s^{-1}}\mathbf{w}_{||\mathrm{R-MF}||}} \tag{21}$$

where $\widehat{\mathbf{R}}^s$ denotes the sample-average estimate of the received signal autocorrelation matrix over $D > J$ signal-of-interest-present snapshots at *SRx*, i.e.

$$\widehat{\mathbf{R}}^s = \frac{1}{D}\sum_{i=0}^{D-1}\mathbf{y}_i\mathbf{y}_i^H. \tag{22}$$

where $\mathbf{y}_i$, $i = 0, 1, \ldots, D-1$ are the available input vectors. Bit decisions are then made over the filtered data as follows

$$\hat{b}_s(P+i) = \mathrm{sgn}(\Re\{\mathbf{w}_{\mathrm{maxSINR}}^H\mathbf{y}_i\}), \quad i = 0, \ldots, J-P-1, \tag{23}$$

where $\mathrm{sgn}\{\cdot\}$ denotes the sign operation.

The SINR attained at the filter output of the secondary receiver, $\mathbf{w}_{\mathrm{maxSINR}}$, for either a narrowband or wideband primary user can be calculated as

$$\begin{aligned}\mathrm{SINR_s} &\stackrel{\triangle}{=} \frac{\mathrm{E}\{|\mathbf{w}_{\mathrm{maxSINR}}^{\mathrm{H}}(\sqrt{\mathrm{E_s}}\mathrm{b_s(P+i)}\mathbf{H}^{\mathrm{ss}}\mathbf{s_s})|^2\}}{\mathrm{E}\{|\mathbf{w}_{\mathrm{maxSINR}}^{\mathrm{H}}(\mathbf{p_i}+\mathbf{n_i})|^2\}} \\ &= E_s\mathbf{s}_s^H{\mathbf{H}^{ss}}^H\mathbf{R}_{I+N}^{s^{-1}}\mathbf{H}^{ss}\mathbf{s}_s = E_s\mathbf{s}_s^H\mathbf{P}_s\mathbf{s}_s \end{aligned} \tag{24}$$

where $\mathbf{P}_s \stackrel{\triangle}{=} {\mathbf{H}^{ss}}^H\mathbf{R}_{I+N}^{s^{-1}}\mathbf{H}^{ss}$, $\mathbf{P}_s \succ 0$. For the case of an all-spectrum wideband primary user, $\mathbf{R}_{I+N}^s$ in (24) is given by

$$\mathbf{R}_{I+N}^s = \sum_{k=1}^{K} E_p\mathbf{Q}_k\mathbf{s}_p\mathbf{s}_p^H\mathbf{Q}_k^H + \sigma_n^2\mathbf{I}_{L+N-1} \tag{25}$$

while for the case of a narrowband primary user $\mathbf{R}_{I+N}^s$ in (24) is given by

$$\mathbf{R}_{I+N}^s = \sum_{k=1}^{K} E_p\mathbf{Q}_k\mathbf{Q}_k^H + \sigma_n^2\mathbf{I}_{L+N-1} \tag{26}$$

where $\mathbf{Q}_k \in \mathbb{C}^{(L+N-1)\times L}$ is the multipath fading channel matrix of the k-th primary user. In practice, we estimate $\mathbf{R}_{I+N}^s$ in (25) and (26) by the sample-average estimate

$$\widehat{\mathbf{R}}_{I+N}^s = \frac{1}{D}\sum_{i=0}^{D-1}(\mathbf{p}_i+\mathbf{n}_i)(\mathbf{p}_i+\mathbf{n}_i)^H \tag{27}$$

where $\mathbf{p}_i$ accounts for the unknown primary users signals and $\mathbf{n}_i$ is complex zero-mean white Gaussian noise.

IV. Proposed Cognitive Channelization Algorithm

In this section we deal with the cognitive decisions that *SRx* needs to communicate to *STx* to achieve cognitive channelization. The objective of our cognitive radio setup is to find an optimal pair of bit energy E_s and real-valued waveform $\mathbf{s}_s \in \mathbb{R}^L$ that maximizes the secondary receiver's post-filtering $\mathrm{SINR_s}$, and at the same time satisfies a primary interference threshold. More specifically, the problem under consideration can be expressed as follows

$$\underset{E_s,\mathbf{s}_s}{\text{maximize}} \ E_s\mathbf{s}_s^T\mathbf{P}_s\mathbf{s}_s \tag{28}$$

$$\text{subject to } E_s\mathbf{s}_s^T\mathbf{P}_p\mathbf{s}_s \le \gamma_p \tag{29}$$

$$E_s\mathbf{s}_s^T\mathbf{P}_s\mathbf{s}_s \ge \gamma_s \tag{30}$$

$$\mathbf{s}_s^T\mathbf{s}_s = 1, \quad 0 < E_s \le E_{max} \tag{31}$$

where $\mathbf{P}_p \stackrel{\triangle}{=} {\mathbf{Q}^{ss}}^H\mathbf{R}_{I+N}^{p^{-1}}\mathbf{Q}^{ss}$, $\mathbf{Q}^{ss}$ is the multipath fading channel matrix for the *STx-PRx* link, $\mathbf{R}_{I+N}^p$ is the disturbance autocorrelation matrix at the primary receiver *PRx*, $\gamma_s > 0$ denotes a minimum acceptable QoS threshold for the secondary link, $\gamma_p > 0$ denotes the primary receiver interference threshold, and E_{max} is the maximum allowable/available bit transmission energy for the secondary user. Both γ_p and γ_s are assumed to be known at the secondary receiver *SRx*. Unfortunately, the optimization task in (28) is non-convex NP-hard (in L) [25].

In the absence of exact knowledge of matrix $\mathbf{P}_p$ of the primary receiver we propose a practically realizable solution that is derived by substituting (29) with an interference temperature

(IT) constraint that is calculated at the secondary receiver. Interference temperature $T_I(f_c, B)$ is specified in Kelvin (K), for a given carrier frequency f_c and bandwidth B, and can characterize both interference and noise in a particular location [26]. More specifically,

$$T_I(f_c, B) \triangleq \frac{P_I(f_c, B)}{kB} \tag{32}$$

where $P_I(f_c, B)$ is the average interference power in Watts, centered at f_c and covering bandwidth of B Hertz. In (32) $k = 1.38 \cdot 10^{-23}$ Joules/K is the Boltzmann's constant.

We assume partial a-priori knowledge of our signal environment (i.e. narrowband or all-spectrum wideband primary transmitters) but no collaboration between the primary and secondary links. Since the primary user does not communicate with the secondary user, we estimate $T_I(f_c, B)$ using the parameter values for f_c and B that we evaluate at the secondary user during its silent periods, as follows

$$\widehat{T}_I(f_c, B) = \frac{1}{kB^2} \int_{f_c - B/2}^{f_c + B/2} S_p(f) \mathrm{d}f \tag{33}$$

where $S_p(f)$ is the power spectral density (PSD) of the primary transmitted signals. Assuming knowledge for the specific frequency band of a tolerable interference limit $T_L(f_c)$ (which, without loss of generality, is equivalent to γ_p), we rewrite the optimization problem in (28) in terms of the IT constraints as follows

$$\underset{E_s, \mathbf{s}_s}{\text{maximize}} \quad E_s \mathbf{s}_s^T \mathbf{P}_s \mathbf{s}_s \tag{34}$$

$$\text{subject to} \quad T_I(f_c, B) + \frac{\mu P_s}{kB} \leq T_L(f_c) \tag{35}$$

$$E_s \mathbf{s}_s^T \mathbf{P}_s \mathbf{s}_s \geq \gamma_s \tag{36}$$

$$\mathbf{s}_s^T \mathbf{s}_s = 1, \quad 0 < E_s \leq E_{max} \tag{37}$$

where $P_s \triangleq \frac{2E_s B}{1+\alpha}$ denotes the transmission power of the secondary transmitter, α is the roll-off factor of the utilized SRRC pulse shaping, and $\mu \in [0, 1]$ represents multiplicative attenuation due to fading and path-loss between the cognitive transmitter (*STx*) and primary receiver (*PRx*).

The optimization problem in (34) becomes separable only if we drop the QoS constraint (36). In addition, the problem is feasible only if the constraint in (36) is satisfied. Thus, the optimal solution in (34), if it exists, is not affected from dropping the secondary QoS constraint. As a result, the optimal transmission power E_s^{opt} for the secondary user is the solution to the following optimization problem

$$\underset{E_s}{\text{maximize}} \quad E_s \mathbf{s}_s^T \mathbf{P}_s \mathbf{s}_s \tag{38}$$

$$\text{subject to} \quad T_I(f_c, B) + \frac{\mu 2E_s}{(1+\alpha)k} \leq T_L(f_c) \tag{39}$$

$$0 < E_s \leq E_{max}. \tag{40}$$

Indeed, we can verify that (39) always holds with equality at an optimal point. Therefore, the optimal transmitting energy can be calculated as

$$E_s^{opt} = \frac{(1+\alpha)k}{2\mu}(T_L(f_c) - T_I(f_c, B)). \tag{41}$$

In the context of this work, the parameter $\mu \in [0, 1]$ is selected empirically based on either the location of the secondary transmitter with respect to the primary receiver (free-space path loss model) or the medium-access-control (MAC) layer characteristics of the primary user link that can be acquired by soft monitoring of the control channel.

By applying (41) to (34) we acquire the optimal waveform $\mathbf{s}_s$ as a solution to the following optimization problem

$$\begin{aligned} \underset{\mathbf{s}_s}{\text{maximize}} \quad & \mathbf{s}_s^T \mathbf{P}_s \mathbf{s}_s \\ \text{subject to} \quad & \mathbf{s}_s^T \mathbf{s}_s = 1. \end{aligned} \tag{42}$$

Let $\mathbf{e}_1, \mathbf{e}_2, \ldots, \mathbf{e}_L$ be the eigenvectors of $\mathbf{P}_s$ with corresponding eigenvalues $\lambda_1 \geq \lambda_2 \geq \cdots \geq \lambda_L$. The normalized waveform $\mathbf{s}_s$ that maximizes $\mathbf{s}_s^T \mathbf{P}_s \mathbf{s}_s$ is the eigenvenctor $\mathbf{s}_s^{opt} = \mathbf{e}_1$ that corresponds to the maximum eigenvalue λ_1 of $\mathbf{P}_s$ [27].

Returning to the problem in (34), we observe that constraint (36) can be satisfied and the problem becomes feasible only if the maximum eigenvalue of $\mathbf{P}_s$, λ_1, is greater or equal to γ_s / E_s^{opt}. If, however, the constraint in (36) is not satisfied, the problem is infeasible and we have to hold off adaptation. This procedure can be repeated in an adaptive fashion by revising the problem in (34) every time the power profile of the primary user changes.

V. Experimental Results

The proposed channelization algorithm is evaluated in an indoor SDR testbed setup. Four $\mathrm{USRP-N210s}$ are deployed in a multipath fading environment (Fig. 3). All four $\mathrm{USRP-N210s}$ interface with $\mathrm{RFX-2400}$ daughtercards that allow full-duplex operation in different carrier frequencies from 2.3 GHz to 2.9 GHz. Figure 3 depicts a secondary link that coexists with either a primary narrowband station or an all-spectrum wideband station both operating at $f_{c_1} = 2.49\,\mathrm{GHz}$. We used GNU Radio to implement both primary and secondary transceiver architectures as well as the proposed cognitive channelization algorithm. For this purpose, we developed custom software signal processing blocks under the GNU Radio API.

Figure 4 summarizes our developments for the implementation of a software-defined all-spectrum cognitive channelization platform. More specifically, the secondary receiver, *SRx*, decodes *STx* frame transmissions in the presence of *PTx* primary signals. During the silent periods of *STx*, the secondary receiver calculates a sample average estimate of $\mathbf{R}_{I+N}^s$ and estimates the interference temperature, denoted as, $T_I(f_c, B)$ of the active primary users. In case that both $\widehat{\mathbf{h}}^{ss}$ and $\widehat{\mathbf{R}}_{I+N}^s$ are available at the secondary receiver (Fig. 4), the

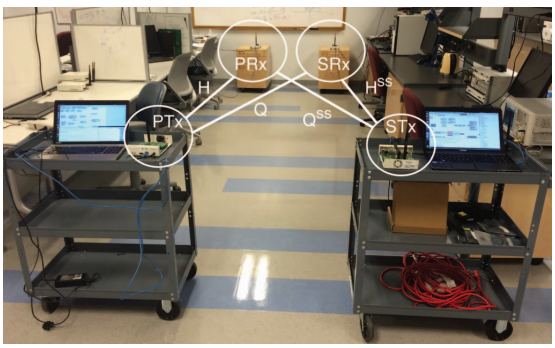

Fig. 3. Indoor SDR testbed setup for all-spectrum cognitive channelization.

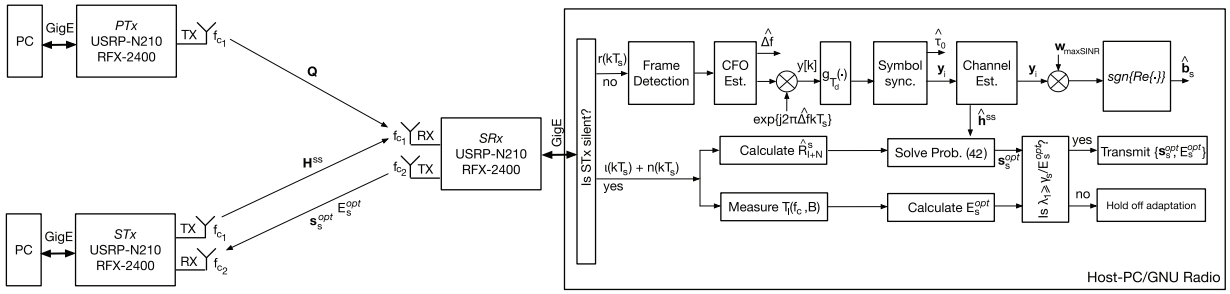

Fig. 4. Overview of the software-defined implementation of the proposed cognitive channelization algorithm with USRP − N210s and GNU Radio.

optimal pair $\{E_s^{opt}, \mathbf{s}_s^{opt}\}$ can be derived and communicated to the secondary transmitter to achieve channelization. The optimal pair of transmission power and channel waveform is communicated to the secondary transmitter via a wireless feedback channel that is established at $f_{c_2} = 2.32$ GHz.

Our experimental setup in Fig. 3 considers two different scenarios, where the primary station is i) a narrowband BPSK system, and ii) an all-spectrum wideband system. For both cases information symbols of secondary users modulate a $L = 15$ randomly selected digital waveform. Narrowband primary transmitters use SRRC pulses of duration $T = 20.48\,\mu s$ while both primary and secondary wideband transmitters use SRRC pulses of duration $T_d = 1.36\,\mu s$. Both narrowband and wideband primary/secondary pulse-shaping filters use $\alpha = 0.35$ roll-off factor. The number of channel paths is set to $N = 3$, while the SINR QoS requirement for the primary users is set to 12 dB (dashed line with triangular markers in Fig. 5(a) and 6(a)). The minimum QoS requirement for the secondary users is set to 26 dB (dashed line with circular markers in Fig. 5(a) and 6(a)). Parameter μ is set equal to 1 to emulate the worst case interference scenario between *STx-PRx*. Our experimental studies are summarized in Fig. 5 and 6 where both SINR and BER performance is depicted at both secondary and primary receivers for different transmission strategies adopted by the secondary users (i.e. cognitive or fixed channelization). The location of both the primary and secondary user, as well as the transmission power and modulation scheme of the primary user are fixed for both experimental scenarios.

Figure 5 demonstrates significant SINR performance improvement for the primary narrowband receiver, when the all-spectrum wideband secondary user decides to cognitively adapt both its transmission power and channel waveform. More specifically, for the fixed channelization case, the secondary user selects its peak available transmission power and the SINR at the primary receiver (*PRx*) drops below its predefined QoS threshold. On the other hand, when cognitive channelization takes place, the secondary user selects its channel waveform in a way that the SINR at the secondary receiver (*SRx*) is maximized, and the interference to the primary link is minimum. As a result, the narrowband link exhibits similar SINR and BER performance as in the case where the secondary user is not present (Fig. 5(a)-(b)). The depicted SINR and BER results are acquired by averaging over a time window of 20 sec (i.e. 2000 packets).

Experimental BER and SINR results for the case of all-spectrum wideband primary and secondary links (Fig. 6) are averaged over a time window of 10 sec (i.e. 1000 packets). To demonstrate the effect of cognitive channelization on system performance, the secondary user is assigned an initial waveform that exhibits high correlation (60%) with the primary user's waveform, emulating this way a high-interference environment. The superior performance characteristics of the proposed channelization algorithm are evident. Compared to fixed channelization, cognitive adaptation of transmission power and waveform at the secondary transmitter results in higher SINR and BER performance at the secondary receiver (*SRx*), as well as improved performance at the primary receiver (*PRx*). As expected, for the case of a narrowband primary link, the SINR

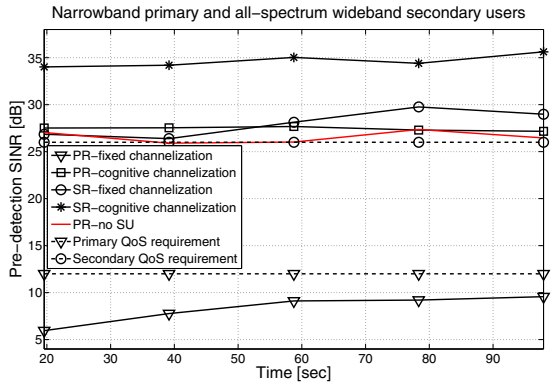

(a) Pre-detection SINR versus time at both primary narrowband and all-spectrum wideband secondary receivers.

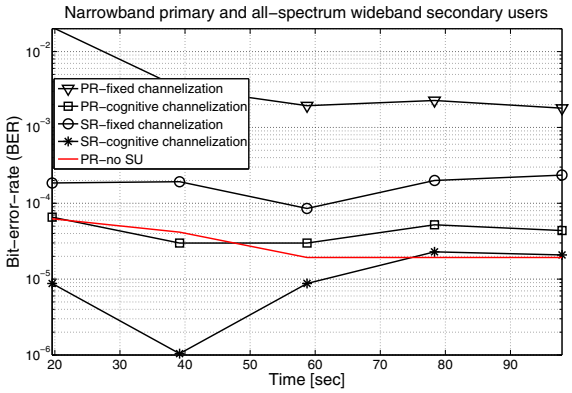

(b) BER versus time at both primary narrowband and all-spectrum wideband secondary receivers.

Fig. 5. Pre-detection SINR (a) and BER (b) measured at both primary narrowband and secondary wideband receivers for the cases of cognitive and fixed channelization. Primary narrowband receiver's SINR and BER are also reported for the case that the secondary transmitter is absent.

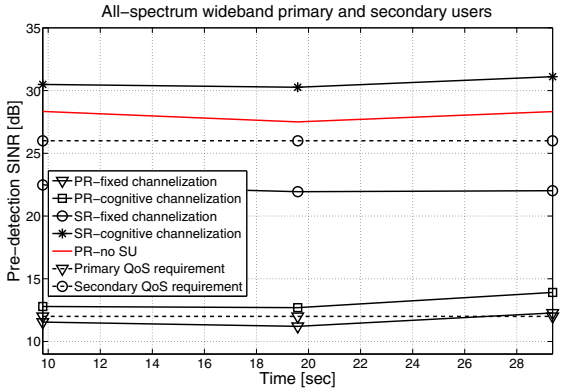

(a) Pre-detection SINR versus time at both primary and secondary all-spectrum wideband receivers.

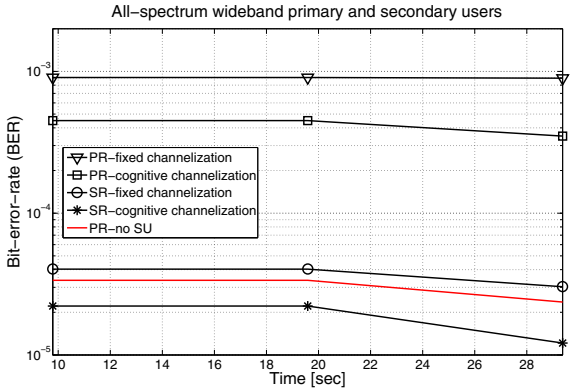

(b) BER versus time at both primary and secondary all-spectrum wideband receivers.

Fig. 6. Pre-detection SINR (a) and BER (b) measured at both primary and secondary all-spectrum wideband receivers for the cases of cognitive and fixed channelization. Primary wideband receiver's SINR and BER are also reported for the case that the secondary transmitter is absent.

and BER performance gains of cognitive channelization are significantly higher than the case of an all-spectrum wideband primary link.

VI. Conclusions

We considered the problem of establishing cognitive all-spectrum secondary links alongside either narrowband or wideband primary users in an indoor SDR testbed. In pursuit of a real-time, non-cooperative solution for optimal secondary link design we imposed interference temperature constraints for the primary link during the optimization process at the secondary receiver and demonstrated a complete testbed for all-spectrum cognitive channelization. Real-time experimental studies demonstrated that cognitive channelization leads to significant performance improvements compared to fixed channelization in terms of SINR and BER at both the secondary and primary receiver.

References

[1] Connecting America: The Nation Broadband Plan (FCC), http://download.broadband.gov/plan/national-broadband-plan.pdf

[2] Federal Communications Commission, Spectrum Policy Task Force, Report ET Docket no. 02-135, Nov. 2002.

[3] I. F. Akyildiz, W. Lee, and K. R. Chowdhury, "CRAHNs: Cognitive Radio Ad Hoc Networks," *Ad Hoc Networks,* vol. 7, pp. 810-836, Jul. 2009.

[4] S. Haykin, "Cognitive radio: Brain-empowered wireless communications," *IEEE Journal on Selected Areas of Communications,* vol. 23, pp. 201-220, Feb. 2005.

[5] K. Gao, O. Ozdemir, D. A. Pados, S. N. Batalama, T. Melodia, and A. L. Drozd, "Cognitive Code-Division Channelization with Admission Control," *Journal of Computer Networks and Communications,* vol. 2012.

[6] K. Gao, S. N. Batalama, D. A. Pados, and J. D. Matyjas, "Cognitive code-division channelization," *IEEE Trans. on Wireless Commun.,* vol. 10, no. 4, Apr. 2011.

[7] L. Ding, K. Gao, T. Melodia, S. N. Batalama, D. A. Pados, and J. D. Matyjas, "All-spectrum cognitive networking through joint distributed channelization and routing," *IEEE Trans. on Wireless Commun.,* pp. 5394–5405, Nov. 2013.

[8] M. Li, S. N. Batalama, D. A. Pados, T. Melodia, M. J. Medley, and J. D. Matyjas, "Cognitive code-division links with blind primary-system identification," *IEEE Trans. on Wireless Commun.,* vol. 10, pp. 3743-3753, Nov. 2011.

[9] R. Zhou, X. Li, V. Chakravarthy, C. Bullmaster, B. Wang, R. Cooper, and Z. Wu "Software defined radio implementation of SMSE based overlay cognitive radio," *Proc. of 2010 IEEE Symposium on New Frontiers in Dynamic Spectrum,* pp. 1-2, Apr. 2010.

[10] R. Zhou, Q. Han, R. Cooper, V. Chakravarthy, and Z. Wu, "A software defined radio based adaptive interference avoidance TDCS cognitive radio," *Proc. of 2010 IEEE International Conference on Communications (ICC),* pp. 1-5, May 2010.

[11] A. Goldsmith, S. Jafar, I. Maric, and S. Srinivasa, "Breaking spectrum gridlock with cognitive radios: An information theoretic perspective," *Proc. of the IEEE,* vol. 97, no. 5, pp. 894-914, May 2009.

[12] Y. Noam and A. J. Goldsmith, "Blind null-space learning for MIMO underlay cognitive radio with primary user interference adaptation," *IEEE Trans. Wireless Commun.,* vol. 12, no. 4, pp. 1722-1734, Dec. 2013.

[13] B. Gopalakrishnan and N. D. Sidiropoulos, "Cognitive Transmit Beamforming From Binary CSIT," *IEEE Trans. Commun.,* vol. 14, no. 2, pp. 895-906, Feb. 2015.

[14] R. Iwata, V. Va, K. Sakaguchi, and K. Araki, "Experiment on MIMO cognitive radio using Tx/Rx beamforming," *Proc. of the 24th IEEE International Symposium on Personal Indoor and Mobile Radio Communications (PIMRC),* pp. 2871-2875, Sept. 2013.

[15] G. Nychis, R. Chandra, T. Moscibroda, I. Tashev, and P. Steenkiste, "Reclaiming the white spaces: Spectrum efficient coexistence with primary users," *Proc. of the 7th COnference on Emerging Networking EXperiments and Technologies (CoNEXT)*, 2011.

[16] H. Rahul, N. Kushman, D. Katabi, C. Sodini, and F. Edalat, "Learning to share: Narrowband-friendly wideband networks," *Proc. of SIGCOMM*, Oct. 2008.

[17] K. Li and H. Liu "Joint channel and carrier offset estimation in CDMA communications," *IEEE Trans. on Signal Process.*, vol. 47, no. 7, pp. 1811-1822, July 1999.

[18] I. N. Psaromiligkos and S. N. Batalama, "Rapid combined synchronization/demodulation structures for DS-CDMA system – Part I: Algorithmic Developments," *IEEE Trans. on Commun.,* vol. 51, no. 6, pp. 983-994, June 2003.

[19] T. Schmidl and D. Cox, "Robust frequency and timing synchronization for OFDM," *IEEE Trans. on Commun.,* vol. 45, no. 12, pp. 1613-1621, 1997.

[20] B. Bloessl, M. Segata, C. Sommer and F. Dressler, "An IEEE 802.11a/g/p OFDM receiver for GNU Radio," *Proc. of the 2nd ACM SIGCOMM Workshop on Software Radio Implementation Forum (SRIF 2013)*, pp. 9-16, Aug. 2013.

[21] E. Sourour, H. El-Ghoroury, and D. McNeill, "Frequency offset estimation and correction in the IEEE 802.11a WLAN," *IEEE VTC*, pp. 4923-4927, Sep. 2004.

[22] S. Haykin, *Adaptive Filter Theory*, 2nd ed. Englewood Cliffs, NJ: Prentice-Hall, 1991.

[23] D. G. Luenberger, Optimization by Vector Space Methods, New York: Wiley, 1969.

[24] A. Bansal, S. N. Batalama, and D. A. Pados, "Adaptive maximum SINR RAKE filtering for DS-CDMA multipath fading channels," *IEEE Journal on Selected Areas in Commun.,* pp. 1765-1773, vol. 16, no. 9, Dec. 1998.

[25] P. M. Pardalos and S. A. Vavasis, "Quadratic programming with one negative eigenvalue is NP-hard," *J. Global Optim.*, vol. 1, pp. 15-22, 1991.

[26] T. Clancy and W. Arbaugh, "Measuring interference temperature," *Proc. Virginia Tech. MPRG Symp. Wireless Personal Commun. (MPRG '06)*, June 2006.

[27] G. N. Karystinos and D. A. Pados, "Rank-2-optimal adaptive design of binary spreading codes," *IEEE Trans. Inform. Theory*, vol. 53, pp. 3075-3080, Sept. 2007.